Absorption and Electroabsorption Spectra of $[(NH_3)_5Ru(4,4'\text{-bipyridine})Ru(NH_3)_5]^{4+}$ in Water by ab Initio Calculations

Ivo Cacelli,[†] Alessandro Ferretti,*[,‡] and Alessandro Toniolo[§]

Scuola Normale Superiore, Piazza dei Cavalieri, I-56126 Pisa, Italy, Istituto di Chimica Quantistica ed Energetica Molecolare del CNR, Area della Ricerca, Via Alfieri 1, I-56010 Ghezzano (PI), Italy, and Dipartimento di Chimica Fisica ed Elettrochimica, Università Milano, Via Golgi 19, I-20133 Milano, Italy

Received: October 6, 2000; In Final Form: February 1, 2001

The absorption spectrum in the visible of $[(NH_3)_5Ru(4,4'\text{-bipyridine})Ru(NH_3)_5]^{4+}$ in water has been studied by extensive multireference configuration interaction calculations. Solvent effects were included by the polarizable continuum model. Size and shape of the cavity surrounding the solute molecule were chosen according to a method that we have previously developed for systems in which solute−solvent hydrogen bonds occur. The dependence of the ground state, as well as that of the first singlet and triplet excited states, has been investigated as a function of the torsion between the two pyridine rings of 4,4′-bipyridine. The line shape profile of the metal-to-ligand charge transfer (MLCT) band has thus been obtained. The modifications of the band due to a static electric field have then been studied, and the possible role of the triplet MLCT state in determining the observed Stark spectrum has been investigated.

Introduction

There is intense activity in the field of donor−bridge−acceptor (DBA) systems aiming at understanding the essential features involved in the through-bridge electron and energy transfer processes,[1−4] which is also stimulated by the possibility of building molecular electronic devices.

DBA systems can be divided in two classes: those that are purely organic, where all three components are organic fragments (see ref 1 and references therein), and those that are inorganic, where D and A are transition metal complexes (see ref 2). These latter are certainly the most suitable candidates for the study of intramolecular electron transfer, since the metals can be tuned in different oxidation states within the molecule, thus allowing a modulation of the electron's flow.

In this perspective, a significant role is played by the organic ligand bridging the metals, first highlighted by Ondrechen et al.[5] for the well-known pyrazine-bridged Ru(II)−Ru(III) dimer (the Creutz−Taube ion),[6] whose delocalized nature has been also recently confirmed by density functional theory (DFT) calculations.[7] In fact, the existence of an empty delocalized ligand orbital, accompanied by a significant metal−ligand interaction, is a key point for an efficient electron delocalization along the whole molecule. These features, plus electronic correlation effects, are of basic importance in the explanation of the observed near-IR−vis optical properties of Ru−pyrazine and Ru−(4,4′-bipyridine) compounds upon oxidation/reduction,[8] well-known indicators of electron localization/delocalization, and in principle should also be relevant for species with different metals and different μ ligands.[9−14]

To rationalize the metal−metal interaction in these compounds, several models were proposed.[8,13−18] In addition, studies of the near-IR−visible optical properties have been carried out by semiempirical[19] or DFT methods.[5,7] However, in view of building a general scheme for the evaluation of metal−metal interaction, it is now well established that a proper description of ligand-bridged metallic dimers can be obtained only taking into account solvent and electronic correlation effects.[20] It is therefore worthwhile to put some effort into performing extensive and accurate multireference configuration interaction (CI) calculations on these systems in solution.

The role played by the solvent in charge transfer metal complexes is well-known and studied.[21] The inclusion of solvent effects in ab initio or semiempirical calculations for metal complexes can be performed in several ways. One can simply consider point charges surrounding the solute,[22a] or take a supermolecule built placing around the solute a small number of solvent molecules[22a,23] and then also add further solvent shells to be dealt with by molecular mechanics (QM/MM methods),[22b,24] or simulate the structure of the solvent around the solute.[25]

We have chosen to employ the polarizable continuum model (PCM) developed by Tomasi and co-workers,[26] which was derived by the Onsager reaction field model,[27] using a specific implementation capable of taking into account the effects of solute−solvent hydrogen bonds. This model is included in a multireference CI description of the solute wave functions.

In previous papers[28] we have investigated the metal-to-ligand charge transfer (MLCT) transition of pyrazine (pyr) and bipyridine (bpy) ruthenium pentaammines in solution of different solvents. In line with the results by less correlated methods,[22,23,25] we have found that only by a proper inclusion of the solvent effects can one obtain reliable predictions of the position of the observed MLCT band. As a matter of fact, our in vacuo calculations predicted transition energies higher of ∼1−1.5 eV with respect to those in solution of polar solvents, for both pyrazine and 4,4′-bipyridine ruthenium pentaammine complexes.[28] Furthermore, as observed experimentally, the red shift

[†] Scuola Normale Superiore. E-mail: ivo@dcci.unipi.it.
[‡] Istituto di Chimica Quantistica ed Energetica Molecolare del CNR. E-mail: ferretti@icqem.pi.cnr.it.
[§] Università Milano. E-mail: toniolo@dcci.unipi.it.

10.1021/jp003676p CCC: $20.00
Published on Web 04/13/2001

of the MLCT band was found to be roughly proportional to the increase of solvent donor number, instead of to its dielectric constant.

With the experience gained so far, we want now to attack the problem of the study of the larger ligand bridged Ru dimers. In particular, we will report here on the study of the absorption spectrum of the title compound as a function of the torsion between the two [Ru(NH_3)$_5$-pyridine] moieties, and also in the presence of a static electric field. This latter is of some importance since the difference of the line shape profile of the MLCT band, with and without the field, represents a probe for the localized/delocalized character of the system.[8f,29,30] The results obtained will be thus compared with the Stark experiments by Boxer et al.,[30] and the hypothesis that spin−orbit coupling is responsible for the observed behavior will be evaluated and discussed.

Method and Computational Details

Our study is based on extensive CI calculations in which solvent effects are included by the PCM method.[26] The whole approach has been widely described in our previous papers,[28] and thus we will repeat here only the main outline.

In PCM the solvent is seen as a polarizable continuum medium with dielectric constant ϵ. The solute molecule, surrounded by a cavity of suitable dimension and shape (representing the solute−solvent interface), polarizes the solvent and thus gives rise to a charge distribution on the cavity surface originating a reaction field potential, $W(\rho_a,\epsilon,\Omega)$. This must be added to the solute electrostatic Hamiltonian in a vacuum H_0. For fixed nuclei one has then to solve the following eigenvalue problem:

$$(H_0 + W(\rho_a,\epsilon,\Omega))|\psi_a\rangle = V_a|\psi_a\rangle \qquad (1)$$

where ρ_a is the electronic + nuclear charge density of the ath state (ψ_a) of the solute and Ω represents the general dependence on the shape and size of the cavity. Once ρ_a is given, the surface density charge is found by imposing definite boundary conditions at the cavity surface,[31] derived by classical electrostatics.

According to eq 1, one should in principle take into account that, upon electronic excitation, the solvent does not have the time to relax from its equilibrium with the ground-state electronic density to that of the excited state. The resulting nonequilibrium problem could be solved within a semiclassical picture,[32−35] but since we have previously found[28a] that this procedure does not bring substantially different values of the transition energies, at least in this class of compounds, we have avoided this complication and solved a simplified version of eq 1:

$$(H_0 + W(\rho_0,\epsilon,\Omega))|\psi_a\rangle = V_a|\psi_a\rangle \qquad (2)$$

where only the reaction field in equilibrium with the ground-state ψ_0 is considered.

It is worthwhile to notice that solute−solvent interactions in the Ru pentaammine compound studied here are expected to involve N−H···O hydrogen bonds. Unfortunately, the PCM, which is based on classical arguments, is in principle unable to adequately treat solute−solvent hydrogen bonds. However, since the electronic excitations under study involve species (Ru and pyz/pyr) far enough from the solute−solvent interface, the problem can be overcome by a proper choice of the shape and dimension of the cavity surrounding the Ru(NH_3)$_5$ fragments. The criteria for the choice of the cavity were already developed and discussed in previous work.[28] Since the ligand bpy does not alter appreciably the NH_3−solvent interaction, we are confident that the cavities optimized in ref 28a for pyrazine can be utilized here without changes. As in ref 28b, in order to have an appropriate shape of the cavity surrounding the pyridine rings of bpy, we have considered one sphere for each C−H of the rings (R = 1.78 Å), centered in the middle of the C−H bond, plus a sphere on the center of each ring (R = 2.90 Å).

With this model for the solvent, we have carried out a PCM-SCF-HF calculation to obtain the best single determinant ψ_0 in solution. In all calculations the 6-31G basis and the 36-electron ECP of Hay and Wadt,[36] with the corresponding DZ basis set for Ru, have been used. Calculations have been performed by using the GAMESS code,[37a] as modified according to ref 37b.

The integrals have then been transformed from atomic to molecular basis, including the one-electron reaction field matrix in equilibrium with the SCF ground state density. In this step we have frozen 48 orbitals and considered the subspace generated by the remaining 50 occupied molecular orbitals (MOs) plus the lowest 50 virtual MOs. All these 100 orbitals have been considered in the multireference (MR) CI calculations in which, following the CIPSI prescriptions, the configuration space is enlarged step by step according to the so-called aimed selection.[38]

The computational procedure can be summarized into four steps. First, a fixed number of eigensolutions is computed for the "zero-order" configuration space S_0. Second, first-order perturbative contribution to the zero-order states by single and double excitations from all Slater determinants of S_0 is computed: a new space called perturbative space (S_p) is built, made by S_0 plus its single and double excitations. Third, a subspace S_η of S_p is selected such that the norm of the first-order correction to the zero-order states is equal to a given value η: η is kept the same for all the desired states and for all the geometries considered and so guarantees the same accuracy. Fourth, the space S_η is added to S_0 and, if the dimension of ($S_0 + S_\eta$) is large enough, the lowest eigensolutions are computed and the sequence stopped, while in the opposite situation the value of η is further decreased and the procedure restarts from the beginning, with ($S_0 + S_\eta$) as the new S_0.

We want to stress further that the selection of the configuration space performed, whose dimension depends on the geometry (the torsion θ in the present case), guarantees that the final eigensolutions have all the same quality (controlled by η). This is useful when one wants to get balanced energies, both for different geometries and for different states, and makes the present approach a valid alternative to more standard MR-CI in which the configuration space is fixed.

For the present work, the variational calculations (CI-V) that we report ranges from 20 000 to 40 000 Slater determinants depending on θ. A second type of CI calculation, the so-called variational-perturbative (CI-VP), has also been performed. This is based on the second-order diagrammatic perturbation[38] using the Epstein−Nesbet (EN) or the Møller−Plesset (MP) schemes. In this case the ($S_0 + S_\eta$) space obtained by a value of η larger than in CI-V calculations (~7000 Slater determinants) is considered for obtaining zero-order states. Then, second-order energy corrections due to the contribution of single and double excitations of all Slater determinants belonging to the ($S_0 + S_\eta$) space are included in the final energies. This latter calculations include the contribution of $\sim 10^{10}$ Slater determinants and, as verified in ref 28b, make the results stable with respect to the choice of the SCF orbitals.

Since, as discussed in detail later in this article, we want also to investigate on the role that the lowest MLCT triplet state

may have in determining the observed Stark spectrum,[30] the spin−orbit matrix elements that couple the strong singlet MLCT with the corresponding spin forbidden triplet transition must be computed. To this purpose we have used an one-electron approximation; that is, the spin−orbit operator is written as an one-electron operator with effective nuclear charges Z^{eff}.[39]

$$\hat{H}_{\text{SO}} = \frac{\alpha}{2}\sum_{i,K}\frac{Z_K^{\text{eff}}}{r_{i,K}^3}(\vec{r}_{\text{i,K}} \times \vec{p}_i)\cdot\vec{s}_i \qquad (3)$$

Indices i and K denote electrons and nuclei respectively, $r_{i,K}$ the electron−nucleus distance, p_i the linear momentum, s_i the spin operator, and α the hyperfine constant. The effective nuclear charges have been computed for the isolated atoms, by a fit of the experimentally known atomic multiplets splitting with full electron spin−orbit calculations. In our case we have considered the following atomic states:

$$\text{C}(^3\text{P}, 2s^2\,2p^2), \text{ whichs give } Z^{\text{eff}} = 3.56$$

$$\text{N}(^4\text{P}, 2s\,2p^4), \text{ which gives } Z^{\text{eff}} = 3.51$$

$$\text{Ru}^{2+}(^5\text{D}, 4d^6), \text{ which gives } Z^{\text{eff}} = 35.62$$

All spin−orbit calculations were carried out without using ECP. To keep the basis to a manageable dimension, a single-ζ basis set was placed on the hydrogen atoms. It was then accurately checked that this simplification does not appreciably alter the molecular electronic distribution of the ground and excited states.

To calculate the line shape profile of the bands due to the inclusion of torsion, we have first computed the torsional wave functions in the Born−Oppenheimer approximation, projecting the eigenvalue problem (in atomic units):

$$\left[-\frac{1}{2I_{\text{R}}}\frac{\text{d}^2}{\text{d}\theta^2} + V_a(\theta)\right]\chi_{ja}(\theta) = E_{ja}\chi_{ja}(\theta) \qquad (4)$$

on a large basis of trigonometric $\cos(k\theta)$ and $\sin(k\theta)$ functions. V_a is the energy of the electronic state ψ_a (eq 2). We have assumed free rotation of each $Ru(NH_3)_5$ group around the Ru−pyr bond; thus the inertia moment I_{R} can be taken as the reduced inertia moment of the two rings with respect to the Ru−N−C−C−N−Ru axis ($I_{\text{R}} \sim 43$ amu Å^2). The quantum photoabsorption cross section (σ_{Q}) is then computed taking into account the statistical population, at room temperature, of the torsional levels of the electronic ground state by

$$\sigma_{\text{Q}}(\omega) = \frac{2\pi^2}{cZ_{\text{Q}}}\sum_{j,m} e^{-E_{j0}/k_{\text{B}}T} f(m1\leftarrow j0)\,\delta(\omega - E_{m1} + E_{j0}) \qquad (5)$$

where E_{j0} and E_{m1} are the energies of the rotational states of the electronic ground-state ψ_0 and excited state ψ_1, respectively, c is the speed of light, and δ is the Dirac delta function. Z_{Q} is the quantum partition function of the internal torsion coordinate ($Z_{\text{Q}} = \sum_j e^{-E_{j0}/k_{\text{B}}T}$). The oscillator strength $f(m1\leftarrow j0)$ is, in the dipole-length approximation

$$f(m1\leftarrow j0) = \frac{2}{3}(E_{m1} - E_{j0})\left|\int \text{d}\theta\, \chi_{j0}^{\,*}(\theta)\, T_{01}(\theta)\, \chi_{m1}(\theta)\right|^2 \qquad (6)$$

where T_{01} is the electronic transition moment between the two electronic states in the dipole approximation.

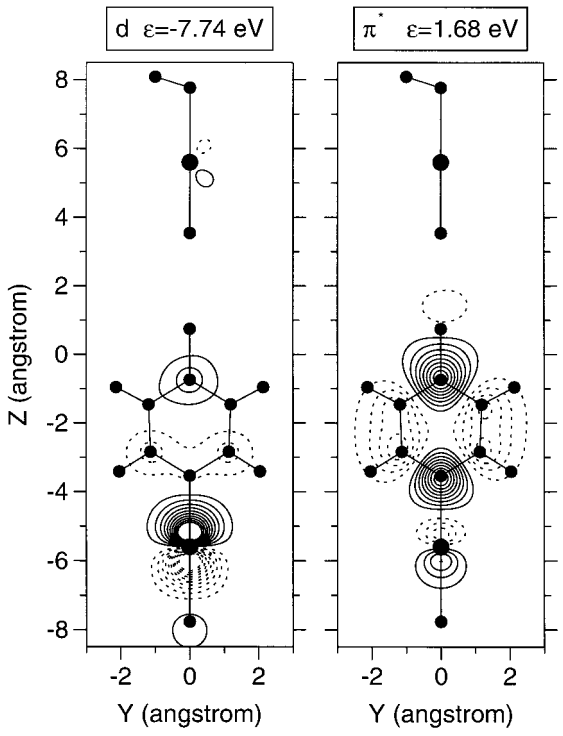

Figure 1. Two-fold degenerate HOMO and LUMO orbitals at $\theta = 90°$. The value of the x coordinate is 0.6 Å. Full line for positive and dashed line for negative values.

The discretized function of eq 5 takes into account the vibronic contribution due to the torsion, neglecting other internal coordinates. This is a strong simplification, since the effect of the other nuclear degrees of freedom, such as the on-site Ru−NH_3 stretch and ring vibrations, as well as Ru−ring vibrations, commonly included in model studies,[8c,f,15e,16,17] is certainly of importance. However, such nuclear motions are not considered here, since an accurate study of the ground and excited potential energy surfaces along several nuclear coordinates would require for the present system a huge quantity of calculations, and is out of the scope of this article. To mimic these effects and obtain a line shape profile, we have then convoluted the cross section of eq 5 with a Gaussian function of fwhm = 0.1 eV. It should also be noticed that, in light of the small spacing of the torsional levels, the classical statistical cross section could also be used (see ref 28b).

Results and Discussion

The effects of solvation by electron-donor solvents in Ru−pentaammine complexes with etheroaromatic ligands was already examined by several methods and extensively discussed.[21−23,25,28] We only remind here that the solvent molecules, as their electron donor capability (donor number) increases, strengthen the electron donation of the ammonia nitrogens and thus increase the electron density on Ru. Therefore, the pseudo t_{2g} d metal orbitals rise in energy while the empty ligand π^* orbital is almost unchanged. The main consequence is a decrease of the MLCT ($d \rightarrow \pi^*$) excitation energies. Furthermore, the solvent also causes a change in the mixing of the occupied and empty π orbitals of the aromatic ligand with the d metal orbitals.[28]

Before going deep into the presentation of the CI results, and in order to get a better understanding of the discussion that follows, it is interesting to look at the relevant SCF orbitals at $\theta = 90°$ (Figure 1) and $\theta = 0°$ (Figure 2). The contour plots refer to a plane parallel to the yz plane at a distance of 0.6 Å along the x coordinate.

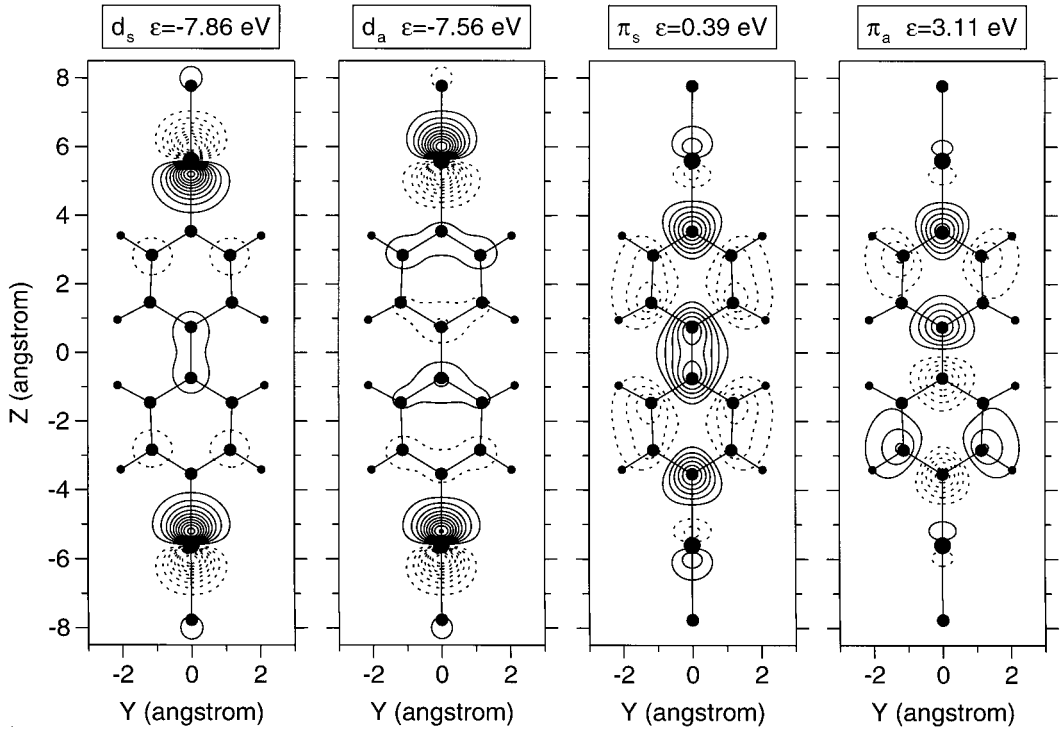

Figure 2. $\theta = 0°$ (the two $Ru[(NH_3)_5]$-pyridine moieties are coplanar). The two orbitals of Figure 1 give rise to the four (symmetric and antisymmetric combinations) shown here.

Neglecting the ammonia groups, when $\theta = 90°$ the molecule belongs to the point group D_{2d} (Figure 1). The HOMO and LUMO orbitals transform according to the doubly degenerate irreducible representation *E*. Both orbitals have a degenerate partner referred to the upper part of the molecule, connected by a rotation of 90° around the *z* axis followed by a reflection in the *xy* plane. The HOMO and LUMO correspond essentially to the d_{xz} of Ru and the π^* of the neighboring pyr and strongly resemble the frontier orbitals of the $[Ru(NH_3)_5-pyr]^{+2}$ compound.

When the two pyr rings of bpy are coplanar ($\theta = 0°$), the molecule belongs to the abelian point group D_{2h}; the degeneracy of the two pairs of orbitals is removed and the four orbitals of Figure 2 are obtained. The two doubly occupied orbitals have both strong metallic character and are the symmetric and antisymmetric combination of Ru d_{xz}'s with minor contributions from the rings. The LUMO (π_s) is essentially the symmetric combination of two π^* orbitals, each centered on one pyr ring. The highest energy orbital (π_a), which is not found by CI to contribute to the visible spectrum, is essentially the antisymmetric combination of two π^* orbitals of pyr. Notice that the three lowest orbitals of Figure 2 strongly resemble the three bonding, nonbonding, and antibonding orbitals of the corresponding pyz compound,[5,7] the only difference being the insertion of the contribution from the π^* orbital of an additional ring in the ligand. It is also worthwhile to notice the strong bonding character of the π_s orbital as far as the two rings are concerned: we will se below that this affects the torsional energy barrier of the excited states involving this orbital.

The ground-state energy as a function of the torsional angle is reported in Figure 3 as obtained by SCF and CI calculations. CI-VP results are given for both the Møller−Plesset (MP) and Epstein−Nesbet (EN) perturbative schemes. At the SCF level there is a minimum (~2 kcal/mol), at about the same angle as in the monomer compound $[Ru(NH_3)_5-bpy]^{2+}$ ($\theta \sim 40°$; ~1.5 kcal/mol),[28b] and a barrier at 90° which is lower than that at 0°. However, in both CI-V and CI-VP calculations the minimum

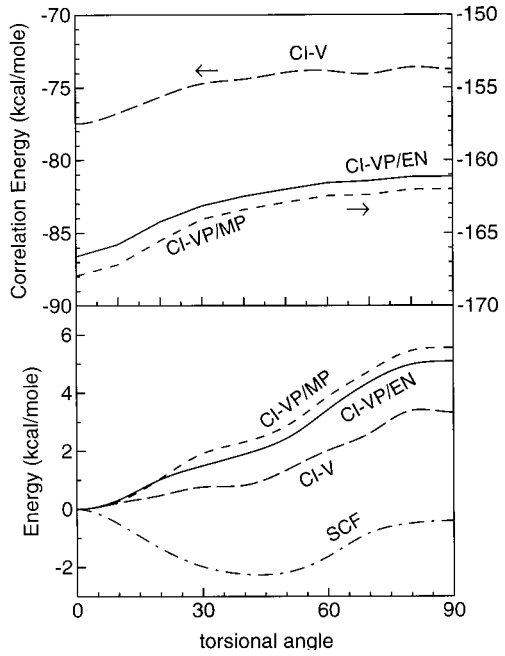

Figure 3. Ground-state energy in water as a function of the torsion (θ) for the various kinds of calculation (lower part). Correlation energy as a function of θ in CI-V (left scale) and CI-VP (right scale) calculations (upper part).

moves to the planar configuration of the two rings ($\theta = 0°$) and an higher barrier is found at $\theta = 90°$. This effect of correlation was already observed, although less intense, in the monomer compound[28b] and finds an explanation in the monotonic decrease, in absolute value, of the correlation energy versus the torsional angle, associated with the corresponding increase of HOMO−LUMO energy gap. Both these effects occur as a consequence of the decrease of electronic delocalization between the two rings when the torsional angle goes from 0° to 90°, which disfavors Ru−ligand back-bonding interaction.

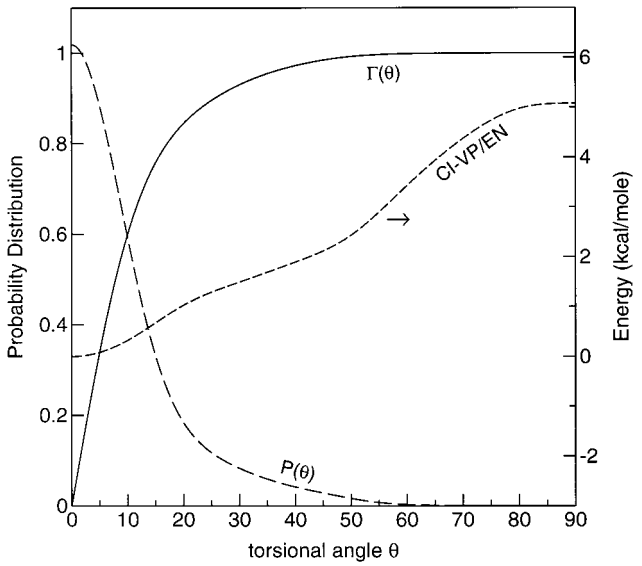

Figure 4. Ground-state probability density distribution (P) and total population (Γ) as a function of θ (left scale). The CI-VP ground-state energy of Figure 3 is also displayed (right scale).

It has to be noticed that a large part of correlation energy is missing in the CI-V calculations (Figure 3, upper part) with respect to those which include a perturbative treatment. This has also the effect of increasing the barrier at 90°. In light of this difference, which makes CI-VP results much more reliable, we will consider only this kind of approach for the computation of the excited states. In particular, we have chosen the EN scheme, since with respect to the MP it is unaffected by the presence of intruder states.

The ground-state probability density distribution ($P(\theta)$) and total population ($\Gamma(\theta)$) as a function of the torsional angle (Figure 4), computed at $T = 273.15$ K according to (see also eq 3)

$$P(\theta) = \frac{\sum_j |\chi_{j0}(\theta)|^2 e^{-E_{j0}/k_B T}}{Z_Q}; \; \Gamma(\theta) = \int_0^\theta P(\theta')\, d\theta' \qquad (7)$$

show that the two rings are in a quasi-planar conformation, as observed in a similar Os compound.[12] In fact (Figure 4), the two rings assume an angle less than 20° with a probability of 80%. Notice also that classical and quantal partition functions are in practice indistinguishable.

Up to 90 kcal/mol above the ground state, several singlet and triplet metal-to-ligand charge transfer (MLCT) excited states involving $d \rightarrow \pi^*$ excitation are found. As expected, only the HOMO → LUMO singlet $d_a \rightarrow \pi_s$ has significant oscillator strength. Moreover, differently from the monometallic species[28] where the difference in $d-\pi^*$ Coulomb and exchange integrals among the three t_{2g} orbitals was significant, this is now the lowest singlet excitation. Its energy (in kcal/mol) and excitation energy (in eV) as a function of the torsion are reported in Figure 5, as obtained by the CI-VP approach described in the previous section (notice that the top and bottom of Figure 5, which apparently look very similar, show respectively the energy of the selected excited states and the corresponding excitation energies, which are the energy differences between the excited and the ground states). In the same figure, also the behavior of the corresponding triplet state is reported, but we do not show the MLCT states that do not have significant oscillator strength and occur at higher energies. This triplet will be considered

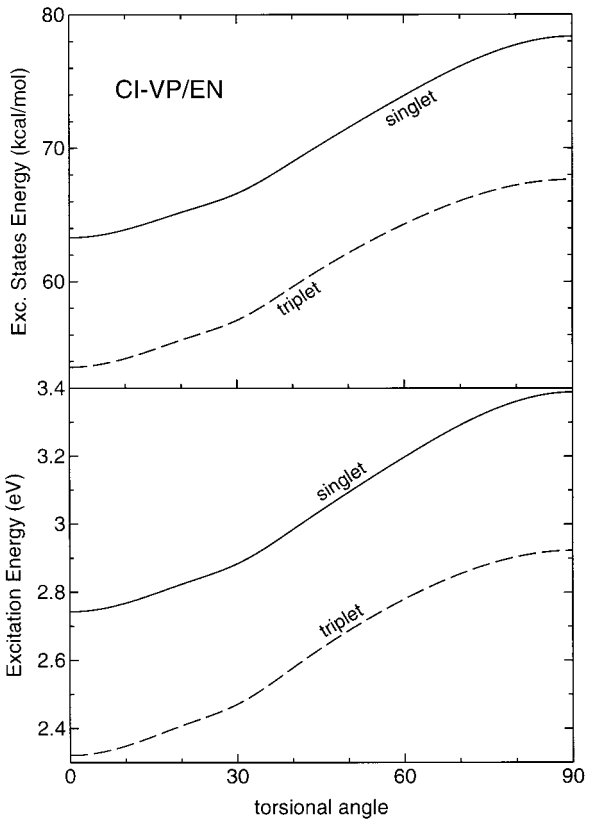

Figure 5. Energy of the $d_{xz} \rightarrow \pi^*$ MLCT singlet and triplet states as a function of θ (upper part): the curves are scaled with respect to the ground-state energy at $\theta = 0°$ ($V_a(\theta) - V_0(0)$). Excitation energies from the ground to the two excited states ($V_a(\theta) - V_0(\theta)$) as a function of the torsion (lower part).

below in our attempt to obtain the Stark spectrum observed experimentally.

The singlet and triplet energy curves show a very similar dependence on the torsion, with a single minimum at 0° and a barrier at 90°. However, the energy grows with θ about twice that in the ground state, and this finds an explanation in the strong bonding character of the π_s orbital between the two pyr rings: since the torsion weakens the ring−ring π bond, the excited states involving the π_s are more stable in the planar conformation. The computed excitation energy is slightly higher than in the experiments, resulting in 2.74 eV at 0° versus the experimental value of ∼2.40 eV;[41] however, the comparison can still be considered satisfactory.

The line shape profile of the MLCT band can be obtained according to eq 6, thus including the broadening due to dependence of the excitation energy on the torsion. To calculate the profile of the electroabsorption spectrum,[30] we have also considered the case of the ion in a static electric field of 4×10^5 V/cm directed along the z axis.

The singlet MLCT excitation (Figure 6, upper part) results in a wide and very symmetric band centered at ∼2.8 eV; width and symmetry are more pronounced than in the parent monomer compound $[(NH_3)_5Ru(4,4'\text{-bpy})]^{2+}$.[28b] In the presence of the electric field the band is displaced to lower energies by ∼0.02 eV, without significant changes in the intensity and in the profile. This results in a difference spectrum with two lobes (Figure 6, lower part), the first positive and the second negative. This does not match properly with the experimental results, in which two additional lobes, one on the red and one, smaller, on the blue, are also observed.[30] That on the red is a clear indication that the MLCT band has two components,[30] while that on the blue

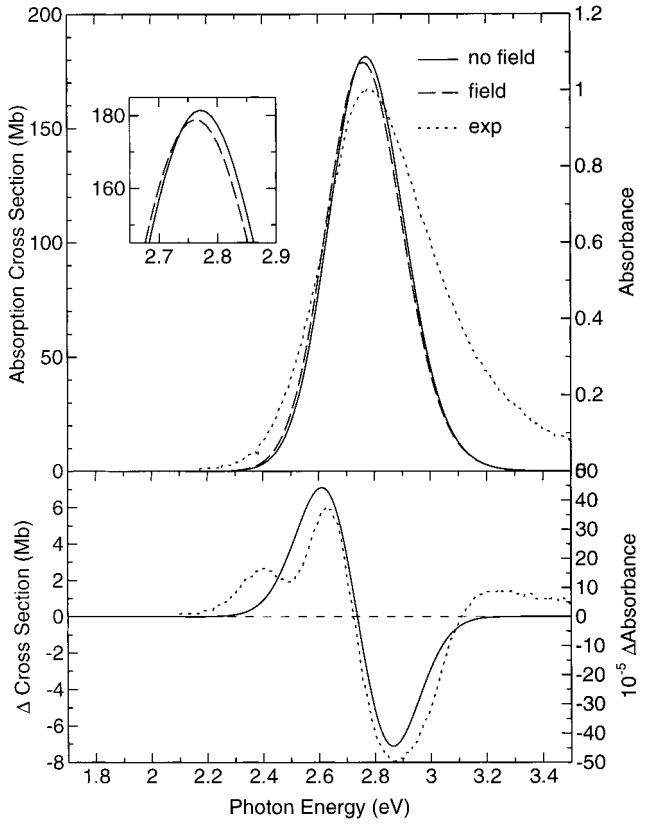

Figure 6. Singlet MLCT band with and without a static electric field of 4×10^5 V/cm (upper part) and corresponding difference spectrum (lower part). (1 Mb = 1 10^{-18} cm^2). Experimental results in glassy water/glycerol matrix at 77 K from ref 30 (dotted line), also reported for comparison, have been shifted by 0.58 eV.

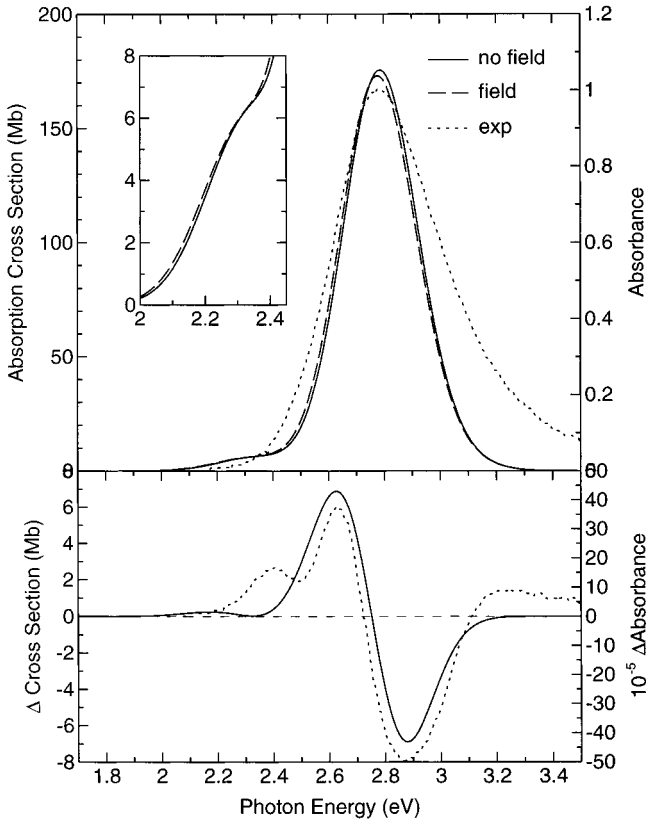

Figure 7. MLCT band with and without a static electric field of 4×10^5 V/cm (upper part) as obtained introducing a phenomenological spin−orbit coupling (see text), and corresponding difference spectrum (lower part). Experimental results in glassy water/glycerol matrix at 77 K from ref 30 (dotted line), also reported for comparison, have been shifted by 0.58 eV.

can be interpreted as a signature of the tendency to electron localization[8f] that can occur only allowing a symmetry breaking along the *z* axis, which was not taken into account in the present calculations.

The existence of a double component of the MLCT band, also identified in the monomer bpy compound but absent when pyrazine replaces bpy, was clearly highlighted in Boxer's paper.[30] Its understanding is of some importance for the comprehension of the optical properties of bpy bridged dimers in the near-IR−visible. In fact, it has been proposed[8e−f] that in this region the spectra can be dominated, for both the homovalent and the mixed-valent species, by MLCT transitions involving different combinations of metallic and ligand π^* orbitals. The model suggesting such an assignment, also predicts a double component MLCT for the homovalent +4 species,[8f] which, however, is not found in the present calculations. This difference unfortunately does not allow a clear understanding of the validity of the model and of its assignment.

We then face two problems. First, since we have only taken into account here a single nuclear degree of freedom, the torsion, can the lack of double component be ascribed to this oversimplification? Second, if this is not the case, what is at the origin of the double component MLCT?

An answer to the first question requires an extensive study of the potential energy surfaces of ground and excited states which, although of extreme importance, is very expensive in terms of computer time. We have decided to postpone such a study to the future and have concentrated our efforts in trying to give an answer to the second question, assuming implicitly a negative answer to the first one.

In this perspective, one can take into account only two possibilities. One is that besides the intense $d_{xz} \rightarrow \pi_s$ MLCT, excitations from the other metallic d orbitals may contribute to the observed band. However, our calculations have shown that the oscillator strengths of the various combinations of $d_{x^2-y^2} \rightarrow \pi_s$ and $d_{yz} \rightarrow \pi_s$ are negligible. Furthermore, these transition are found at too high energies and this possibility can thus be rejected. The second is that a mixing between singlet and triplet $d_{xz} \rightarrow \pi_s$ MLCT occurs, as a consequence of spin−orbit coupling. Indeed, the triplet MLCT state is found about 0.4 eV below the singlet (Figure 5) and could then reasonably be responsible for the double component we are looking for.

To investigate on this possibility, we have first considered a phenomenological spin−orbit coupling of 650 cm^{-1} (0.08 eV), as taken from the literature for the corresponding pyrazine compound.[42] Such a small coupling has the effect of mixing the singlet and triplet MLCT states with negligible changes in their energies. With that value we obtain the absorption and electroabsorption spectra of Figure 7. The line shape profile of the band shows a tail in the red region due to the triplet that borrows oscillator strength from the singlet. This is absent in the experimental absorption spectrum.[30] However, it should be considered that the experimental width is reasonably greater than that of our computations, probably as a consequence of the oversimplification in retaining only the torsion and neglecting all other sources of broadening.

As far as the electroabsorption spectrum is concerned, the computed profile now shows the positive lobe on the red region also present in the Boxer experiment of ref 30, which is the signature of the double component MLCT.

We have then decided to go further and compute ab initio,

with the method described in the previous section (i.e., without using ECPs), the value of the spin−orbit coupling between the singlet and triplet $d_a \rightarrow \pi_s$ MLCT transitions. The values obtained are very small: for instance using the variational states obtained by a CI space of about 8000 Slater determinants, we get a coupling of only 0.4 cm^{-1}, and thus the spin−orbit coupling has a negligible effect on the spectrum. Furthermore, the dependence of the computed spin−orbit coupling on the dimension of the variational CI space, as well as on improvements of the one-electron basis set, is very small. The spectrum of Figure 7, which appears to give an explanation for the experiment, does not have then the support of ab initio arguments.

Since at present we are unable to evaluate the reliability of the method utilized for the computation of spin−orbit coupling, we do not feel able to give a definitive answer to this problem.

Conclusions

With the present article we begin an ab initio study of the near-IR−visible optical properties of ligand bridged ruthenium dimers in solution. The approach utilized is that of extensive multireference CI, and solvent effects, which have proven to play a significant role, are included by the PCM method.

Here we have focused on the homovalent +4 Ru pentaammine dimer with 4,4′-bipyridine as bridging ligand, much less studied than its pyrazine companion, but somehow more interesting for its tendency to show electron localization, as demonstrated by the Stark experiments of ref 30.

Investigating the effects of the torsion between the two pyridine rings of 4,4′-bipyridine, we have found, at CI level, that both ground and excited MLCT states have a single minimum at $\theta = 0°$. This angular dependence results in a symmetric line shape of the MLCT band, as observed in the experiments. Furthermore, the position of the band itself is found in rather good agreement with the experimental value in water[41] (∼2.8 versus ∼2.4 eV).

Going further in the study, we have investigated the response of the spectrum to the action of a static electric field. The electroabsorption (Stark) spectrum computed taking into account the intense singlet MLCT band alone does not show the behavior observed experimentally, i.e., that of a two-component band. We have then evaluated the possibility that spin−orbit coupling may give rise to an intensity borrowing leading to two components in the MLCT absorption. This hypothesis has shown to bring substantial improvement in the agreement with the experiments when a phenomenological value of the spin−orbit coupling is taken. However, an attempt to calculate ab initio the value of this coupling has brought a value too small to be significant. Since we are unable to evaluate the reliability of this kind of computations, we do not feel able to draw any definite conclusion on this point.

Acknowledgment. We acknowledge the kind help of Drs. Chiara Cappelli and Benedetta Mennucci (Chemistry Department, University of Pisa) in providing us their modified version of GAMESS.

References and Notes

(1) Davis, W. B.; Svec, W. A.; Ratner, M. A.; Wasielewski, M. R. *Nature* **1998**, *396*, 60.

(2) Balzani, V.; Scandola, F. *Supramolecular Photochemistry*; Horwood: Chichester, UK, 1991.

(3) Newton, M. D. *Chem. Rev.* **1991**, *91*, 767.

(4) Barbara, P. F.; Meyer, T. J.; Ratner, M. A. *J. Phys. Chem.* **1996**, *100*, 13148.

(5) (a) Zhang, L.-T.; Ko, J.; Ondrechen, M. J. *J. Am. Chem. Soc.* **1987**, *109*, 1666.

(6) (a) Creutz, C.; Taube, H. *J. Am. Chem. Soc.* **1969**, *91*, 3988. (b) Creutz, C. *Prog. Inorg. Chem.* **1983**, *30*, 1.

(7) Bencini, A.; Ciofini, I.; Daul, C. A.; Ferretti, A. *J. Am. Chem. Soc.* **1999**, *121*, 11418.

(8) (a) Ferretti, A.; Lami, A. *Chem. Phys.* **1994**, *181*, 107. (b) *Chem. Phys. Lett.* **1994**, *220*, 327. (c) Ferretti, A.; Lami, A.; Ondrechen, M. J.; Villani, G. *J. Phys. Chem.* **1995**, *99*, 10484. (d) Erratum. *J. Phys. Chem.* **1996**, *100*, 20174. (e) Ferretti, A.; Lami, A.; Villani, G. *Inorg. Chem.* **1998**, *37*, 2799. (f) Ferretti, A.; Improta R.; Lami, A.; Villani, G. *J. Phys. Chem. A* **2000**, *42*, 9591. (g) Denti, G.; Ferretti, A.; Sommovigo, M. Submitted.

(9) (a) Sutton, J. E.; Taube, H. *Inorg. Chem.* **1981**, *20*, 3125. (b) Kim, Y.; Lieber, C. M. *Inorg. Chem.* **1989**, *28*, 3990. (c) Woitellier, S.; Launay, J.-P.; Spangler, C. W. *Inorg. Chem.* **1989**, *28*, 758. (d) Ribou, A. C.; Launay, J.-P.; Takahaschi, K.; Nihira, T.; Tarutani, S.; Spangler, C. W. *Inorg. Chem.* **1994**, *33*, 1325.

(10) Lay, P. A.; Magnuson R. H.; Taube, H. *Inorg. Chem.* **1988**, *27*, 2364.

(11) Hornung, M. F.; Bauman, F.; Kaim, W.; Olabe, J. A.; Slep, L. D.; Fiedler, J. *Inorg. Chem.* **1998**, *37*, 311.

(12) Demadis, K. D.; Neyhart, G. A.; Kober, E. M.; White, P. S.; Meyer, T. J. *Inorg. Chem.* **1999**, *38*, 5948.

(13) (a) Watzky, M. A.; Macatangay, A. V.; Van Camp, R. A.; Mazzetto, S. E.; Song, X.; Endicott, J. F. *J. Phys. Chem.* **1997**, *101*, 8441. (b) Macatangay, A. V.; Endicott, J. F.; Song, X. *J. Phys. Chem. A* **1998**, *102*, 7537. (c) Endicott, J. F.; Macatangay, A. V. *Inorg. Chem.* **2000**, *39*, 437.

(14) Crutchley, R. J., *Adv. Inorg. Chem.* **1994**, *41*, 273.

(15) (a) Allen, G. C.; Hush, N. S. *Prog. Inorg. Chem.* **1967**, *8*, 357. (b) Hush, N. S. *Prog. Inorg. Chem.* **1967**, *8*, 391. (c) Reimers, J. R.; Hush, N. S. *Inorg. Chem.* **1990**, *29*, 3686. (d) Reimers, J. R.; Hush, N. S. *Inorg. Chem.* **1990**, *29*, 4510. (e) Reimers, J. R.; Hush, N. S. *Chem. Phys.* **1996**, *208*, 177.

(16) (a) Piepho, S. B.; Krausz, E. R.; Schatz, P. N. *J. Am. Chem. Soc.* **1978**, *100*, 2996. (b) Piepho, S. B. *J. Am. Chem. Soc.* **1988**, *110*, 6319. (c) Piepho, S. B. *J. Am. Chem. Soc.* **1990**, *112*, 4197.

(17) Ondrechen, M. J.; Ko, J.; Zhang, L.-T. *J. Am. Chem. Soc.* **1987**, *109*, 1672.

(18) Cave, R. J.; Newton, M. D. *Chem. Phys. Lett.* **1996**, *249*, 15.

(19) (a) Sizova, O. V.; Baranovski, V. I.; Ivanova, N. V.; Panin, A. I. *Int. J. Quantum Chem.* **1997**, *63*, 853. (b) Sizova, O. V.; Baranovski, V. I.; Ivanova, N. V.; Panin, A. I. *Russ. J. Coord. Chem.* **1998**, *24*, 219. (c) Metcalife, R. A.; Vasconcellos, L. C. G.; Mirza, H.; Franco, D. W.; Lever, A. B. P. *J. Chem. Soc., Dalton Trans.* **1999**, *118*, 2653. (c) Masui, H.; Freda, A. L.; Zerner, M. C.; Lever, A. B. P. *Inorg. Chem.* **2000**, *39*, 141.

(20) Hush, N. S.; Reimers, J. R. *J. Phys. Chem.* **1999**, *103*, 3066.

(21) Chen, P.; Meyer, T. J. *Chem. Rev.* **1998**, *98*, 1439.

(22) (a) Stavrev, K. K.; Zerner, M.; Meyer, T. J. *J. Am. Chem. Soc.* **1995**, *117*, 8684. (b) Pearl, G. M.; Zerner, M. *J. Am. Chem. Soc.* **1996**, *118*, 2059.

(23) Shin, Y. K.; Brunschwig, B. S.; Creutz, C.; Newton, M. D.; Sutin, N. *J. Phys. Chem.* **1996**, *100*, 1104.

(24) (a) Warshel, A. *J. Phys. Chem.* **1979**, *83*, 1640. (b) Luzhkov, V.; Warshel, A. *J. Am. Chem. Soc.* **1991**, *113*, 4491.

(25) (a) Zeng, J.; Hush, N. S.; Reimers, J. R. *J. Am. Chem. Soc.* **1996**, *118*, 2059. (b) Zeng, J.; Hush, N. S.; Reimers, J. R. *J. Phys. Chem.* **1996**, *100*, 19292.

(26) (a) Tomasi, J.; Persico, M. *Chem. Rev.* **1994**, *94*, 2027. (b) Tomasi, J.; Mennucci, B.; Cammi, R.; Cossi, M. In *Computational Approaches to Biochemical Reactivity*; Nárayt-Szabó, G., Warshel, A., Eds.; Kluwer Academic: Amsterdam, 1997; pp 1−102.

(27) Onsager, L. *J. Am. Chem. Soc.* **1936**, *58*, 1486.

(28) Cacelli, I.; Ferretti, A. *J. Chem. Phys.* **1998**, *109*, 8583. Cacelli, I.; Ferretti, A. *J. Phys. Chem.* **1999**, *103*, 4438.

(29) (a) Reimers, J. R.; Hush, N. S. *J. Phys. Chem.* **1991**, *95*, 9773. (b) Murga, L. F.; Ferretti, A.; Lami, A.; Ondrechen, M. J.; Villani, G. *Inorg. Chem. Commun.* **1998**, *1*, 137. (c) Ferretti, A.; Lami, A.; Murga, L. F.; Shehadi, I. A.; Ondrechen, M. J.; Villani, G. *J. Am. Chem. Soc.* **1999**, *121*, 2594.

(30) Oh, D. H.; Sano, M.; Boxer, S. G. *J. Am. Chem. Soc.* **1991**, *113*, 6880.

(31) Mennucci, B.; Tomasi, J. *J. Chem. Phys.* **1997**, *106*, 5151.

(32) Lee, S.; Hynes, J. T. *J. Chem. Phys.* **1988**, *88*, 6853.

(33) Kim, H. J.; Hynes, J. T. *J. Chem. Phys.* **1990**, *93*, 5194.

(34) Aguilar, M. A.; Olivares del Valle, J.; Tomasi, J. *J. Chem. Phys.* **1993**, *98*, 7375.

(35) Cammi, R.; Tomasi, J. *Int. J. Quantum Chem.* **1995**, *29*, 465.

(36) Hay, P. J.; Wadt, W. R. *J. Chem. Phys.* **1985**, *82*, 270; *J. Chem. Phys.* **1985**, *82*, 284; *J. Chem. Phys.* **1985**, *82*, 299.

(37) (a) Schmidt, M. W.; Baldridge, K. K.; Boats, J. A.; Elbert, S. T.; Gordon, M. S.; Jensen, J. H.; Koseki, S.; Matsunaga, N.; Nguyen, K. A.; Su, S. J.; Windus, T. L.; Dupuis, M.; Montgomery, J. A. *J. Comput. Chem.* **1993**, *14*, 1347. (b) Mennucci, B.; Toniolo, A.; Cappelli, C. *J. Chem. Phys.* **1999**, *111*, 7197.

(38) (a) Cimiraglia, R. *J. Chem. Phys.* **1985**, *83*, 1746. (b) Angeli, C.; Cimiraglia, R.; Persico, M.; Toniolo, A. *Theor. Chem. Acc.* **1997**, *98*, 57. (c) Angeli, C.; Persico, M. *Theor. Chem. Acc.* **1997**, *98*, 117.

(39) Abegg, P. W. *Mol. Phys.* **1975**, *30*, 579.

(40) (a) Ribeiro da Silva, M. A. V.; Morais, V. M. F.; Matos, M. A. R.; Rio, C. M. A. *J. Org. Chem.* **1995**, *60*, 5291. (b) Ould-Moussa, L.; Poizat, O.; Castellà-Ventura, M.; Buntinx, G.; Kassab, E. *J. Phys. Chem.* **1996**, *100*, 2072.

(41) Creutz, C.; Chou, M. H. *Inorg. Chem.* **1987**, *26*, 2995.

(42) (a) Neuenschwander, K.; Piepho, S. B.; Schatz, P. N. *J. Am. Chem. Soc.* **1985**, *107*, 7862. (b) Ko, J.; Zhang, L.-T.; Ondrechen, M. J. *J. Am. Chem. Soc.* **1986**, *108*, 1712.